CSYS Final Project

Modeling the pharmacodynamics of L-Dopa treatments and associated inhibitory enzymatic reactions to optimize dosing regimens.

Cam Lunn[1] and Will Wright[2]
[1]Complex Systems and Data Science, [2]Department of Electrical and Biomedical Engineering

Abstract:

Parkinson's Disease (PD) is one of the most prevalent neurodegenerative diseases across the world causing a disruption in motor function. Although generally asymptomatic in early stages, progression of the disease leads to accumulation of motor dysfunction including bradykinesia, tremors, muscle stiffness, and more. There are currently no cures, but pathology of PD is mostly understood. Neurodegeneration of cells in the substantia nigra region of the brain causes loss of dopamine-producing neurons. Furthermore, neurons of the substantia nigra lose the ability to communicate with neurons of the basal ganglia, resulting in the loss of motor function. The gold standard of treatment is dopamine replacement therapy (DRT), which uses the precursor molecule levodopa (L-dopa) to be synthesized into dopamine. The main problem with DRT is the variability among patient responses to treatment. Furthermore, the side effects of treatment can be too adverse for a patient to continue treatment. This can largely be attributed to misprocessing of L-dopa by the host's metabolome. Thus, it is crucial to understand the pharmacodynamic landscape of L-dopa and further elucidate the dynamical processes intervening in the delivery of levodopa into the substantia nigra. A multiscale pharmacodynamic analysis of various steps in the levodopa pathway were implemented. Models included comparisons of Rytary and Sinemet (brands of carbidopa/levodopa), selegiline inhibitor models, and dopamine biosynthesis models. Results indicate that the pharmacodynamics of levodopa and related enzymatic reactions can be visualized, quantified, and compared on a relative basis, with the potential to more precisely simulate physiological processes with the addition of experimental data. These findings, although generalized, may help optimize dosing regimens of L-dopa treatments for patients with Parkinson's Disease.

Background:

As the second most common neurodegenerative disease, 90,000 individuals are diagnosed with Parkinson's Disease (PD) every year in the United States. In total, there are around 1,000,000 individuals living with PD in the U.S, and is considered to be a key contributor to disability across the world[1-4]. A 2015 study aggregated data from 1990 to 2015, and identified that the number of individuals affected by PD has doubled[5]. By 2030, cases are expected to reach 1,200,000 in the US alone - a 20% increase in incidence from 2022 data[1]. Furthermore, it is estimated that a total $52 billion in economic burden is attributed to PD related costs[6,7].

Parkinson's disease is commonly known as an aging-related disease. As such, the prevalence of PD increases across age groups[1-8]. In a meta-analysis from 2014, the prevalence in individuals under the age of 50 is 41 per 100,000 people, whereas 1903 per 100,000 people in individuals over the age of 80[8]. Besides age as a risk factor, geographic location and sex have shown to be risk factors in PD incidence[1,2]. Both incidence and prevalence of PD are associated with a 1.5 to 2.0 times increased risk for males compared to females[3]. Additionally, incidence rates are generally higher in regions where industrial chemicals and manufacturer are more prevalent (i.e. Rust Belt)[1].

Symptoms associated with Parkinson's vary. In the early stages, patients can exhibit tremors, loss of smell, sleeping problems, dizziness and fainting, and many other symptoms[9]. With lack of unique symptoms attributed to early stages of PD, it is difficult to diagnose. Thus, incorporating the history of the patient's family regarding any neurological disorders can be useful. Even for medial to late stages of PD, clinical symptoms are the main diagnostic technique. The main symptom is bradykinesia, which is a general slowness of movement exhibited by the patient[10]. This must be accompanied by one or more additional symptoms, such as severe tremors, trouble maintaining balance, and/or difficulty maintaining (straight) posture[11,12]. Some imaging techniques like CT, MRI, or DaTscans scans can be ordered, but are seldom effective and are only adjunctly utilized to confirm clinical diagnosis[13].

As a neurological disease impacting motor control, Parkinson's Disease is caused by the accumulation of degenerated neurons in the substantia nigra region of the brain[14]. The substantia nigra produces the neurotransmitter dopamine, which is the essential component of communication between the substantia nigra and basal ganglia[14-16]. This interneuronal communication is essential for movement exhibited by multicellular organisms[12,14]. Over the course of aging, PD pathology manifests when the nerve cells of the substantia nigra lose their dopamine-producing function. In accordance, the

quantity of available dopamine diminishes[14]. Once a threshold of ~70-80% of substantia nigra exhibits loss of function, symptoms manifest and diagnosis is possible[17].

Due to the lack of dopamine producing neurons in the substantia nigra, one of the main treatments is known as dopamine replacement therapy (DRT)[12,18,20]. Dopamine is a highly polar molecule which prevents the neurotransmitter from directly crossing the blood-brain barrier (BBB)[19]. Thus, using the dopamine-precursor molecule called Levodopa (L-Dopa) is the gold standard for DRT[18,20-22]. The enzyme Aromatic L-Amino acid Dopa Decarboxylase (AADC) synthesizes dopamine from L-Dopa that has entered the brain. When treating with L-Dopa, starting doses are small and are slowly increased in increments depending on patient symptoms and response. However, the path from L-Dopa to dopamine is complicated by other pathways competing for the bioconversion of the precursor molecule. This leads to the requirement of other adjuvant drugs to complement the effects of L-dopa.

In the PNS, other dopa decarboxylases (DDCs) will convert L-Dopa to dopamine before it can reach the BBB. Thus, peripheral dopamine decarboxylase inhibitors (i.e. Carbidopa) are frequently administered in conjunction with L-dopa to prevent the premature conversion - allowing more L-dopa to pass the BBB and be converted into dopamine[23]. An additional limitation is catechol O-methyltransferase (COMT), an enzyme which deactivates and degrades L-Dopa both in the PNS and the CNS[25]. Thus, the use of COMT inhibitors is another essential strategy to maintain faithful L-dopa delivery and synthesis of dopamine in the brain[26]. In the CNS, another enzyme is monoamine oxidase B (MAO-B), which functions to regulate and catabolize certain neurotransmitters, including dopamine[27]. MAO-B inhibitors block the catabolism of dopamine, enhance dopamine signaling, and are frequently used in treatment as well[28]. One particular MAO inhibitor is selegiline, which preferentially inhibits MAO-B at low doses and prevents metabolism of dopamine[29,31]. Considering the MAO-B, COMT, and decarboxylase inhibitors, the delivery and bioconversion of L-dopa to dopamine is challenging.

Depending on the patient and their ability to tolerate side effects, a combination of these drugs can be administered. However, ideal dosing regimens are not well understood, and side effects can be severe. Depending on the patient's age and molecular profile, L-dopa can cause severe nausea, dizziness, headaches, hallucinations, psychosis, and other neurological side effects[24]. Many of these symptoms are due to metabolic conversion of L-dopa by the DDCs in the PNS, for which carbidopa can be utilized. Carbidopa is a DDC inhibitor incapable of crossing the BBB, blocks L-dopa conversion to dopamine in the PNS, and results in an increased potency of L-dopa absorption into the CNS[30]. As such, levodopa and carbidopa are administered in tandem to increase

efficiency of treatment. Sinemet is an orally administered drug which combines both L-dopa and carbidopa into one capsule. Thus, the carbidopa improves the potency of L-dopa whilst mitigating the adverse symptoms from it[32]. Rytary, similar to Sinemet, combines both carbidopa and levodopa. Specifically, Rytary uses the ratio of 4:1 levodopa to carbidopa[33]. Unique to Rytary is the split of immediate release to extended release, which is a one third to two thirds split respectively[34]. Both drugs have been proven effective, but dosing titrations are still not well understood on a per patient basis[35].

By modeling the pharmacodynamics of L-dopa absorption, we can understand the effects of differing dosage regimens on the rate of absorption. For model simplicity, only selegiline, carbidopa, and levodopa are considered. Figure 1 depicts the relationship between these three drugs.

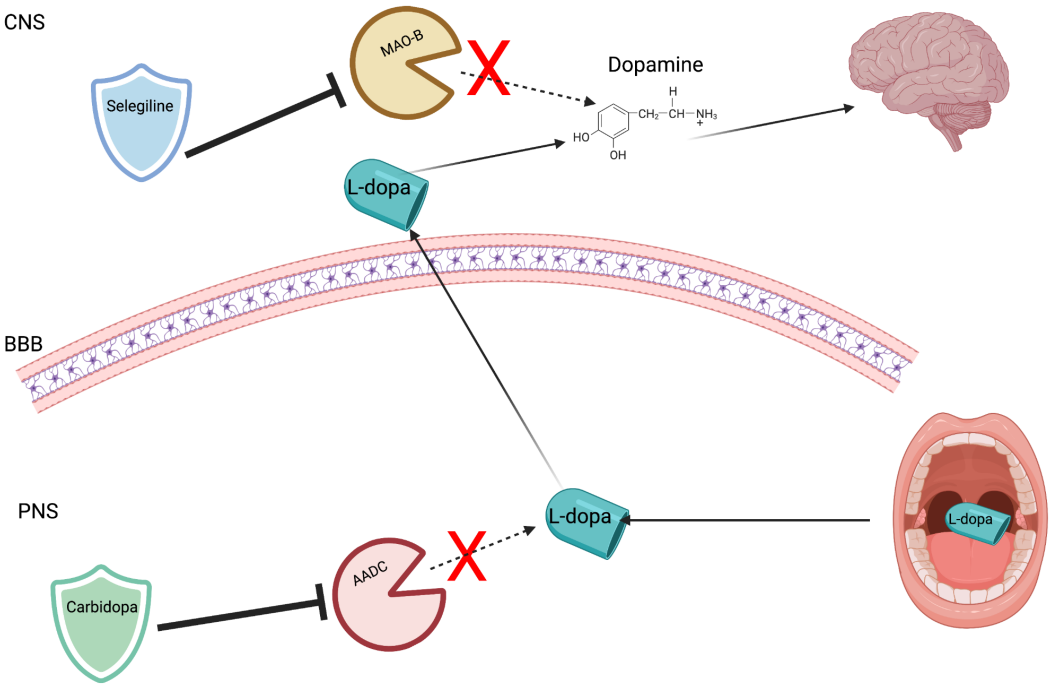

Figure 1. Simplified pharmacokinetic landscape of L-dopa passing the blood brain barrier (BBB). In the PNS, carbidopa inhibits the decarboxylase activity from the AADC enzyme, preventing the premature conversion of the precursor molecule to dopamine. This allows the transfer of L-dopa across the BBB, where it is converted into dopamine by other decarboxylases. MAO-B enzymes function to mark dopamine for degradation, but selegiline inhibits MAO-B molecules. Thus, dopamine accumulates and begins relieving some of the motor function distress in the patient.

Results/Methods

Github Repo

Note: SimBiology Model Builder code cannot be saved. Schematic networks are included as images to show models.

Generation of Figures

Figure 1 was created in Bio Render. Figure 2 was generated using Biopython v1.75, and using .pdb files downloaded from Protein Data Bank. Figures 3-8 were generated in SimBiology Model Builder from MATLAB applications.

Protein Representations

Of primary interest are the main proteins involved in the pharmacogenomics of Parkinson's Disease. As such, the following proteins were analyzed: Human monoamine oxidase B (MAO-B); Human dopa decarboxylase (DDC); Human catechol O-Methyltransferase (COMT). To begin with, the 3-dimensional structures predicted from the AlphaFold database are illustrated below in Figure 1.

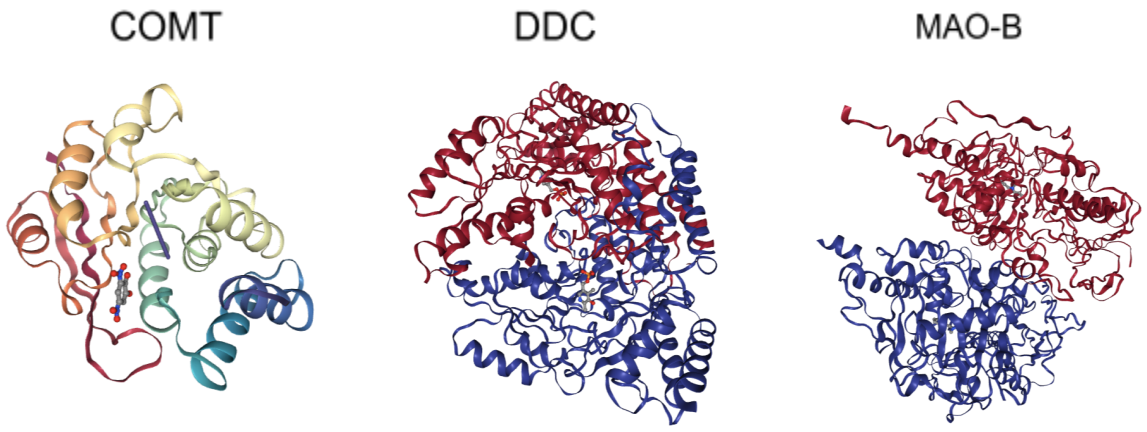

Figure 2. AlphaFold representations of COMT, DDC, and MAO-B proteins show structures mainly composed of alpha helices. The alpha helices form string-like arms, which may highlight each protein's ability to bind to dopamine directly, or its precursor protein L-Dopa (for DDC). Interestingly, AlphaFolds prediction of COMT's

structure is low in comparison to DDC and MAO-B. Proteins imported from the .pdb files from the RCSB Protein Data Bank using Biopython v1.75. The following Protein Data Bank Structures were used: 1GOS (MAO-B); 1JS2 (DDC); 3BWM (COMT).

The pharmacodynamics of levodopa in the periphery and central nervous system are dependent on a myriad of factors related to dosing regimen, absorption, metabolic activity, and elimination dynamics. By using computational models to simulate individual reaction kinetics, we can optimize dosing schedules and maximize the concentration of levodopa available for conversion to dopamine in the brain. The models were created using MATLAB 2022b SimBiology Model Builder and Analyzer software. Two compartments were added to represent the periphery and the central nervous system, with a junction between them to represent the blood brain barrier. Rytary controlled release (CR) capsules and Sinemet CR capsules were administered into the model at 97.5 mg 3x a day (at 60% potency – equivalent to 58.5 mg of levodopa) and 100 mg 2x a day followed by one 50 mg dosage at night, respectively. This regimen follows standard dosing cycles described by Prescriber's Digital Reference[39]. Levodopa pathway schematics were constructed for both Rytary and Sinemet, following the same general flow pattern from administration to elimination of the respective drug. Reaction rates (orange nodes) and dosage schedules were varied based on findings in the literature, or were arbitrarily chosen and set equal between the two models if no information was available.

Each orange node represents a rate of loss or diffusion of levodopa and can be adjusted as needed depending on the initial conditions. For instance, Rytary has been experimentally shown to have an elimination rate that is approximately 2.5x slower than CR Sinemet capsules, and is reflected by the node accordingly[40] .

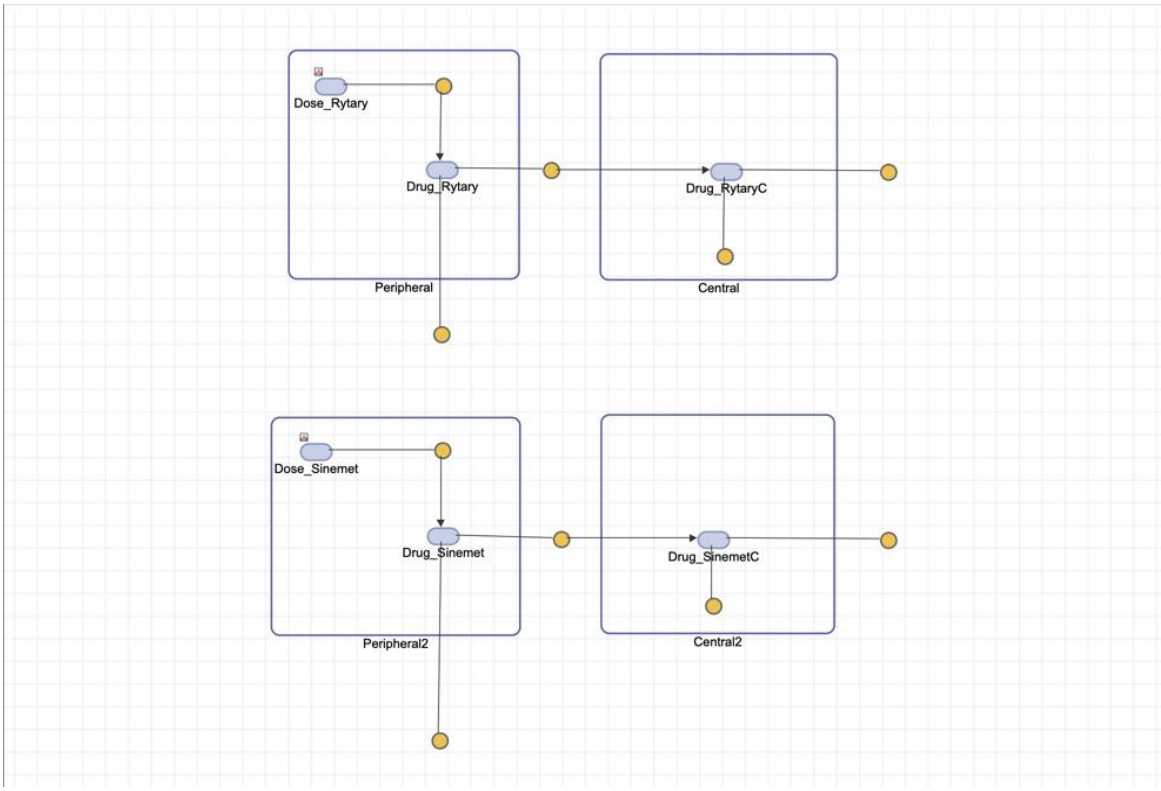

Figure 3. Schematics of levodopa flow for Rytary and Sinemet. Peripheral and Central compartments represent the periphery (blood) and central nervous system (brain). The gap between compartments represents the BBB and yellow nodes represent rates of reaction and diffusion. Rates and dosages are changeable parameters dependent on outside metabolic reactions and dosing regimens.

The bioavailability of levodopa is also dependent on metabolic activity in the periphery and central nervous system and can be further altered by introducing drugs such as Selegiline, which increases the concentration of available levodopa. To account for these modifications, separate schematics were created to model the inhibitory behavior of the previously mentioned inhibitory drugs. Figure 4 shows the schematic for Selegiline targeting MAO-B and the corresponding dynamics of inactive metabolite production with and without Selegiline in Figure 4. Instead of acting as a competitor to MAO-B by binding to levodopa itself, Selegiline specifically targets MAO-B and prevents the enzyme from converting levodopa into inactive metabolites.

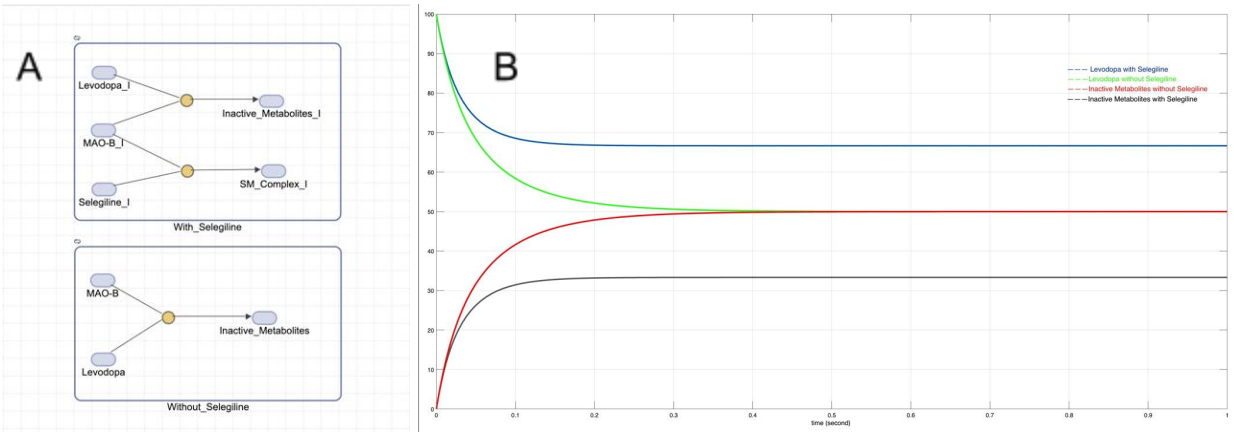

Figure 4. Enzymatic reaction of levodopa, MAO-B, and MAO-B inhibitor (Selegiline). (A) Schematic of MAO-B and levodopa interaction with and without Selegiline. **(B)** Plot showing the relative levels of levodopa and inactive metabolite with and without Selegiline. All nodes are assigned the same rate so that the interaction is generalized and relative. Blue: Levodopa with Selegiline; Green: Levodopa without Selegiline; Red: Inactive metabolites without Selegiline; Black: Inactive metabolites with Selegiline.

A simplified schematic of carbidopa was also included using a reversible node to simulate the inhibitory effect that carbidopa has on levodopa to dopamine conversion. The forward reaction is assigned the same rate in each model, with the reverse rate being less than the forward rate and arbitrarily chosen to reflect general inhibitory kinetics. Initial doses of levodopa were chosen to be 100 mg for each schematic to best visualize the inverse dynamics of levodopa and dopamine levels in the periphery for cases with and without carbidopa.

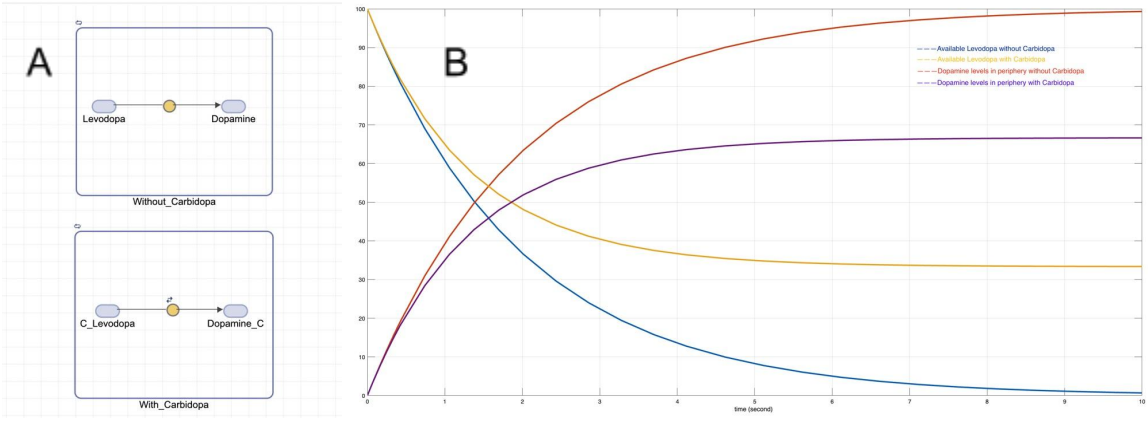

Figure 5. Conversion of levodopa to dopamine, with and without carbidopa. **(A)** Schematic of levodopa to dopamine conversion in the periphery without and with the presence of carbidopa. **(B)** A plot illustrating the levels of levodopa and dopamine in the periphery with and without carbidopa. Dopamine is not useful in the periphery as it cannot pass the BBB. Blue: Available levodopa without Carbidopa; Yellow: Available levodopa with Carbidopa; Red: Dopamine levels in periphery without Carbidopa; Purple: Dopamine levels in periphery with Carbidopa.

The resulting pharmacodynamics of Rytary and Sinemet were plotted for a 2-day period given the standard dosing regimens described in the schematics (Figure 2). Levels of levodopa are shown in three parts, as portrayed in Figures 5 and 6. The blue curves represent the dosage at each time interval, the pink curves represent the levels of levodopa in the periphery, and the black curves represent the levels of levodopa in the central nervous system for conversion to dopamine. The dosing regimens assumed a waking period from 8 am (initial dose, indicated at t = 0) to 12 am (bedtime dose) with an 8-hour period for rest in a normal 24-hour day. The dosing schedule for Rytary consisted of 3 equally spaced administrations of 58.5 mg of levodopa over a 24-hour period (starting at t = 0) and repeated for each subsequent day. The dosing schedule for Sinemet followed 3 equally spaced administrations of levodopa (starting at t = 0), with 100 mg administered for the first 2 intervals and 50 mg administered for the last. Figure 5 shows the complete dosing regimen for Rytary and Figure 6 for Sinemet. The x-axis denotes time (in hours) and the y-axis (not labeled) represents levodopa levels in mg.

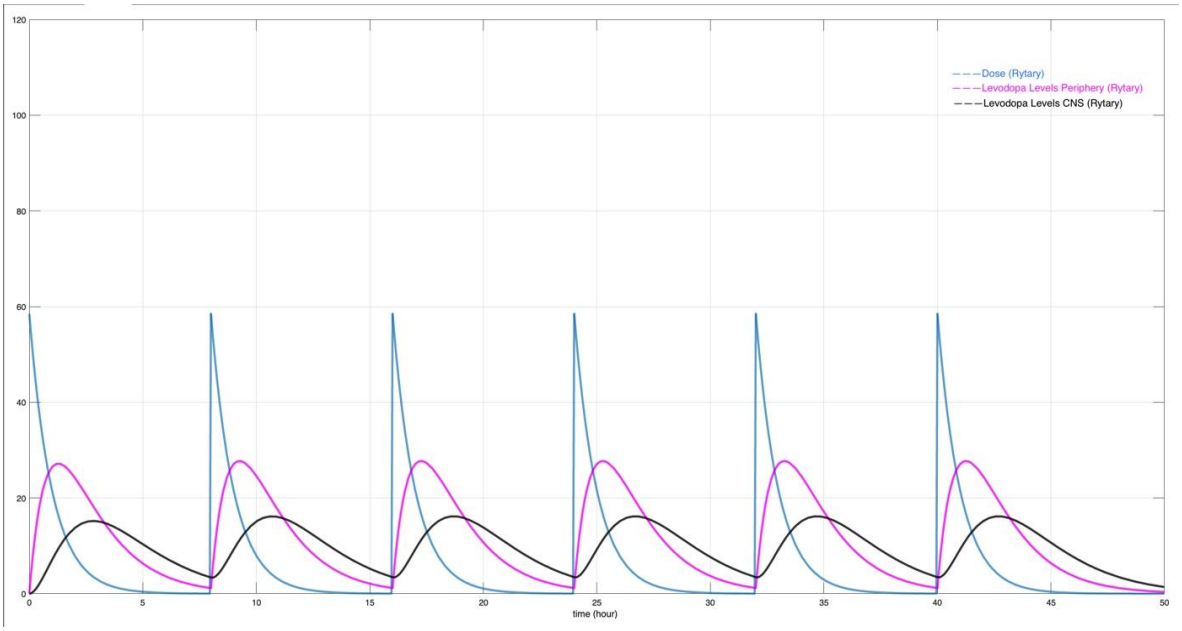

Figure 6. Dosing regimen and levodopa levels in the periphery and central nervous system for Rytary. Total levodopa administered over the 2-day period → 351 mg. Blue: Rytary dosage; Purple: Levodopa levels in periphery (Rytary); Black: Levodopa levels in the CNS (Rytary).

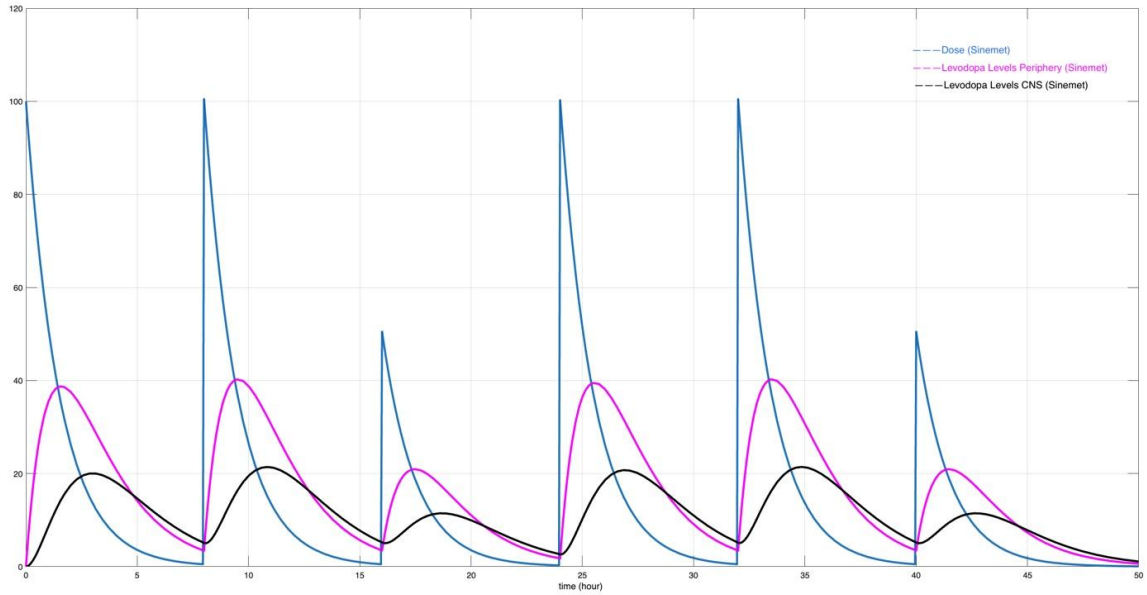

Figure 7. Dosing regimen and levodopa levels in the periphery and central nervous system for Sinemet. Total levodopa administered over the 2-day period → 500 mg. Blue: Sinemet dosage; Purple: Levodopa levels in periphery (Sinemet); Black: Levodopa levels in the CNS (Sinemet).

The levels of levodopa in the central nervous system via Rytary and Sinemet were also compared to investigate the kinetic properties of the two dosing schedules. The dosing regimen for Sinemet displayed greater fluctuations in levodopa levels with the highest local maximum and lowest local minimum concentration, excluding the tails of initial and final dosages. The curves of the Rytary regimen are more consistent, reaching a steady fluctuation cycle after the first several hours. Total levodopa administered in the form of Rytary over the 2-day period was 351 mg, and 500 mg for Sinemet.

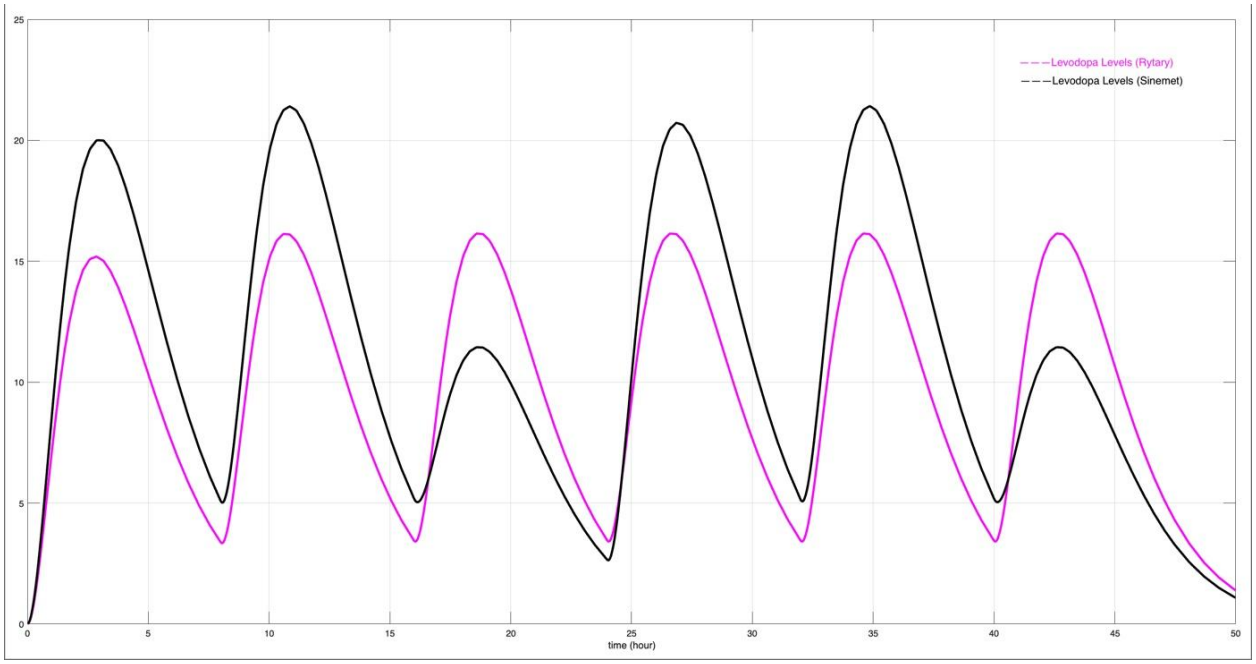

Figure 8. Levels of levodopa in the CNS for Rytary and Sinemet dosing regimens over a 2-day period. Levodopa levels of Sinemet exhibit a dip in the usual peak between 16 and 24 hours, whereas Rytary is consistent. Pink: Levodopa levels (Rytary); Black: Levodopa levels (Sinemet).

Discussion

The enzymatic reactions of Selegiline and carbidopa, as illustrated in Figures 4 and 5, provide metrics for the general levodopa schematic in Figure 3. This schematic uses arbitrary elimination and diffusion rates which allow for relative comparisons between dosing regimens. However, a more biologically accurate model of levodopa pharmacodynamics can be achieved by incorporating values derived from the individual metabolic reactions. For instance, the rate of elimination of available levodopa in the periphery, represented by the node outside the peripheral compartment in Figure 3, is largely decided by carbidopa concentration and inhibition as described in Figure 5. Given known concentrations of carbidopa and levodopa, the carbidopa schematic can be used to determine the rate for the elimination node in the Figure 3 schematic.
The same can be done for Selegiline, simulated using the schematic shown in Figure 4. Introducing a known dosage of Selegiline into a system with known concentrations of MAO-B and dopamine will provide relative rates that can be assigned to the inner and outer nodes of the central compartment in the Rytary and Sinemet schematics. Determining biologically accurate reaction rates requires experimentation, however, estimates can be made purely based on the relative abundance of dopamine and/or

inactive metabolites in the brain with and without Selegiline. The nodes resting in the BBBs of the main schematics would also reflect a diffusion rate of only about 0.01 in an accurate model, as ~1% of available levodopa in the periphery makes it to the brain[41].

The dynamics of levodopa in the CNS (Figure 8) reflect the different dosing regimens of Sinemet and Rytary. With regards to PD related symptoms, the Sinemet dosing schedule may display higher peak levels of levodopa, however, the more pronounced fluctuations imply more significant “off” periods in which returning symptoms feel more severe. The total amount of levodopa administered in the Sinemet dosing regimen was 500 mg versus the 351 mg administered in the Rytary regimen. While no integration was done to evaluate the efficiency of each regimen, the Rytary dosing schedule appears to maintain comparable and more consistent levodopa levels relative to the amount of total levodopa administered. This is likely due in part to the elimination rate, which is approximately 2.5x slower with Rytary than it is with Sinemet. It is also important to consider the levels of levodopa present upon waking up, as it is generally advantageous to employ a regimen that allows for some baseline concentration of levodopa to be present in the body at the beginning of the day. Both regimens follow a similar lower limit trend with no baseline parameters defined in this model.

The model presented can be used as a tool to optimize dosing regimens for individual PD patients. In applying this method, the patient and neurologist would work together to define parameters that address the patient's needs. Possible parameters include limiting fluctuations (the “off” period), increasing peak levodopa concentration, meeting baseline waking levodopa levels, decreasing/increasing intervals of administration, and limiting general doses among other requirements. Current methods for implementing and changing levodopa treatment plans are highly arbitrary and usually entail increasing the amount of levodopa intake, often exacerbating negative side effects such as constipation, nausea, and dizziness. While modeling the pharmacodynamics of levodopa still relies on experimental data and simplifications/assumptions related to reaction rates, it is one step towards achieving personalized, quantitatively-based medicine.

Some limitations to these models is the overarching simplification of the actual biological processes. For purposes of generalization, human catechol O-Methyltransferases (COMT) was omitted, along with many other relevant enzymes. In other words, all models analyzed the pharmacodynamic effects of one inhibitor’s interactions with L-dopa at a time, which does not capture the network complexity of actual biological systems.

Some future directions to further optimize dosing regimens should consider more molecular components, as well as mutations that are prevalent in the general population. Mutations exist in COMT genes which can alter the effects of DRT. One polymorphism, the Val158Met mutation, occurs frequently in the Caucasian population at a minor allele frequency of 0.5. Furthermore, the resulting enzyme can have increased, intermediate, or low metabolizing ability - resulting in high variation in treatment response by DRT[36,37]. Thus, dosage titrations should be adjusted based on an individual's unique molecular profile. Other molecular players in L-dopa delivery to the CNS include transporter proteins, which play an essential role in the absorption and elimination of L-dopa. The gene SLC22A1, which encodes the Organic Cation Transporter 1 (OCT1) protein, exhibits a SNP (rs622342) that was found to be associated with a higher required dose of anti-Parkinson's drugs[38]. Presumably there are many other mutations, such as in the AADC gene, which affect the biosynthesis of dopamine from L-dopa.

The models proposed in this paper are general, and assume no mutations like the aforementioned exist. In order to optimize dosage regimens, an improved understanding of each patient's molecular profile is key. Otherwise, the drug could be rendered ineffective by a patient's metabolome - or even pose harmful side effects.

References

1. *Statistics*. (n.d.). Parkinson's Foundation. https://www.parkinson.org/understanding-parkinsons/statistics

2. *Parkinson's Disease – Symptoms, Diagnosis and Treatment*. (n.d.). https://www.aans.org/en/Patients/Neurosurgical-Conditions-and-Treatments/Parkinsons-Disease

3. Lampropoulos, I., Malli, F., Sinani, O., Gourgoulianis, K. I., & Xiromerisiou, G. (2022). Worldwide trends in mortality related to Parkinson's disease in the period of 1994–2019: Analysis of vital registration data from the WHO Mortality Database. *Frontiers in Neurology*, *13*. https://doi.org/10.3389/fneur.2022.956440

4. Dorsey, E. R., Elbaz, A., Nichols, E., Abd-Allah, F., Abdelalim, A. A., Adsuar, J. C., Ansha, M. G., Brayne, C., Choi, J. J., Collado-Mateo, D., Dahodwala, N., Phuc, H., DO, Edessa, D., Endres, M., Fereshtehnejad, S., Foreman, K. J., Gankpé, F. G., Gupta, R., Hankey, G. J., . . . Murray, C. J. L. (2018). Global, regional, and national burden of Parkinson's disease, 1990–2016: a systematic analysis for the Global Burden of Disease Study 2016. *Lancet Neurology*, *17*(11), 939–953. https://doi.org/10.1016/s1474-4422(18)30295-3

5. Feigin, V. L., Abajobir, A. A., Abate, K. H., Abd-Allah, F., Abdulle, A. M., Abera, S. F., Abyu, G. Y., Ahmed, M. B., Aichour, A. N., Aichour, I., Aichour, M. T. E., Akinyemi, R., Alabed, S., Al-Raddadi, R., Alvis-Guzman, N., Amare, A. T., Ansari, H., Anwari, P., Ärnlöv, J., . . . Disorders, G. N. (2017). Global, regional, and national burden of neurological disorders during 1990–2015: a systematic analysis for the Global Burden of Disease Study 2015. *Lancet Neurology*, *16*(11), 877–897. https://doi.org/10.1016/s1474-4422(17)30299-5

6. Willis, A. W., Roberts, E., Beck, J. D., Fiske, B. K., Ross, W., Savica, R., Van Den Eeden, S. K., Tanner, C. M., Marras, C., Alcalay, R., Schwarzschild, M., Racette, B., Chen, H., Church, T., Wilson, B., & Doria, J. M. (2022). Incidence of Parkinson disease in North America. *Npj Parkinson's Disease*, *8*(1). https://doi.org/10.1038/s41531-022-00410-y

7. Yang, W., Hamilton, J. L., Kopil, C., Beck, J. D., Tanner, C. M., Albin, R. L., Dorsey, E. R., Dahodwala, N., Cintina, I., Hogan, P. F., & Thompson, T. (2020). Current and projected future economic burden of Parkinson's disease in the U.S. *NPJ Parkinson's Disease*, *6*(1). https://doi.org/10.1038/s41531-020-0117-1

8. Pringsheim, T., Jette, N., Frolkis, A. D., & Steeves, T. (2014). The prevalence of Parkinson's disease: A systematic review and meta-analysis. *Movement Disorders*, *29*(13), 1583–1590. https://doi.org/10.1002/mds.25945

9. *The National Council on Aging*. (n.d.). https://www.ncoa.org/article/parkinsons-disease-early-signs-symptoms-and-what-to-do-when-diagnosed

10. Berardelli, A., Rothwell, J., Thompson, P. D., & Hallett, M. (2001). Pathophysiology of bradykinesia in Parkinson's disease. *Brain*, *124*(11), 2131–2146. https://doi.org/10.1093/brain/124.11.2131

11. Reichmann, H. (2010). Clinical Criteria for the Diagnosis of Parkinson's Disease. *Neurodegenerative Diseases*, *7*(5), 284–290. https://doi.org/10.1159/000314478

12. *Getting Diagnosed*. (n.d.). Parkinson's Foundation. https://www.parkinson.org/understanding-parkinsons/getting-diagnosed

13. Gilbert, R. (2022). What is a DaTscan and should I get one? *American Parkinson Disease Association*. https://www.apdaparkinson.org/article/what-is-a-datscan-and-should-i-get-one/

14. Triarhou, L. C. (2013). *Dopamine and Parkinson's Disease*. Madame Curie Bioscience Database - NCBI Bookshelf. https://www.ncbi.nlm.nih.gov/books/NBK6271/

15. Pickel, V. M., Beckley, S., Joh, T. H., & Reis, D. J. (1981). Ultrastructural immunocytochemical localization of tyrosine hydroxylase in the neostriatum. *Brain Research*, *225*(2), 373–385. https://doi.org/10.1016/0006-8993(81)90843-x

16. Freund, T. F., Powell, J., & Smith, A. D. (1984). Tyrosine hydroxylase-immunoreactive boutons in synaptic contact with identified striatonigral neurons, with particular reference to dendritic spines. *Neuroscience*, *13*(4), 1189–1215. https://doi.org/10.1016/0306-4522(84)90294-x

17. El-Agnaf, O. M. A., Salem, A. Z., Paleologou, K. E., Curran, M. D., Gibson, M. A., Court, J. A., Schlossmacher, M. G., & Allsop, D. (2006). Detection of oligomeric forms of α‐synuclein protein in human plasma as a potential biomarker for Parkinson's disease. *The FASEB Journal*, *20*(3), 419–425. https://doi.org/10.1096/fj.03-1449com

18. Ferrazzoli, D., Carter, A., Ustun, F. S., Palamara, G., Ortelli, P., Maestri, R., Yücel, M., & Frazzitta, G. (2016). Dopamine Replacement Therapy, Learning and Reward Prediction in Parkinson's Disease: Implications for Rehabilitation. *Frontiers in Behavioral Neuroscience*, *10*. https://doi.org/10.3389/fnbeh.2016.00121

19. M Burnham, P., & Gregory, S. (2008, October). *Dopamine - Molecule of the Month October 2008 - HTML-only version*. http://www.chm.bris.ac.uk/motm/dopamine/dopamineh.htm#:~:text=This%20is%20because%20the%20dopamine,contains%20the%20chemical%20L%2Ddopa.

20. Pringsheim, T., Day, G. S., Smith, D., Rae-Grant, A., Licking, N., Armstrong, M. J., De Bie, R. A., Roze, E., Miyasaki, J. M., Hauser, R. A., Espay, A. J., Martello, J., Gurwell, J. A., Billinghurst, L., Sullivan, K. L., Fitts, M. A., Cothros, N., Hall, D. A., Rafferty, M. R., . . . Lang, A. E. (2021). Dopaminergic Therapy for Motor Symptoms in Early Parkinson Disease Practice Guideline Summary. *Neurology*, *97*(20), 942–957. https://doi.org/10.1212/wnl.0000000000012868

21. Redenšek, S., Bizjan, B. J., Trošt, M., & Dolžan, V. (2019). Clinical-Pharmacogenetic Predictive Models for Time to Occurrence of Levodopa Related Motor Complications in Parkinson's Disease. *Frontiers in Genetics*, *10*. https://doi.org/10.3389/fgene.2019.00461

22. Corvol, J., & Poewe, W. (2017). Pharmacogenetics of Parkinson's Disease in Clinical Practice. *Movement Disorders Clinical Practice*, *4*(2), 173–180. https://doi.org/10.1002/mdc3.12444

23. Dumbhare, O., & Gaurkar, S. S. (2023). A Review of Genetic and Gene Therapy for Parkinson's Disease. *Cureus*. https://doi.org/10.7759/cureus.34657

24. Gandhi, K. R. (2022, May 2). *Levodopa (L-Dopa)*. StatPearls - NCBI Bookshelf. https://www.ncbi.nlm.nih.gov/books/NBK482140/

25. Goetz, C. G. (1998). Influence of COMT inhibition on levodopa pharmacology and therapy. *Neurology*, *50*(Issue 5, Supplement 5), S26–S30. https://doi.org/10.1212/wnl.50.5_suppl_5.s26

26. *COMT Inhibitors*. (n.d.). Parkinson's Foundation. https://www.parkinson.org/living-with-parkinsons/treatment/prescription-medications/comt-inhibitors

27. Tan, Y., Jenner, P., & Chen, S. (2022). Monoamine Oxidase-B Inhibitors for the Treatment of Parkinson's Disease: Past, Present, and Future. *Journal of Parkinson's Disease*, *12*(2), 477–493. https://doi.org/10.3233/jpd-212976

28. Chen, J., & Swope, D. M. (2005). Clinical Pharmacology of Rasagiline: A Novel, Second-Generation Propargylamine for the Treatment of Parkinson Disease. *The Journal of Clinical Pharmacology*, *45*(8), 878–894. https://doi.org/10.1177/0091270005277935

29. Mazumder, M. K., Paul, R., Phukan, B. C., Dutta, A., Chakrabarty, J., Bhattacharya, P., & Borah, A. (2018). Garcinol, an effective monoamine oxidase-B inhibitor for the treatment of Parkinson's disease. *Medical Hypotheses*, *117*, 54–58. https://doi.org/10.1016/j.mehy.2018.06.009

30. Leyden, E. (2022, July 22). *Carbidopa*. StatPearls - NCBI Bookshelf. https://www.ncbi.nlm.nih.gov/books/NBK554552/#:~:text=Carbidopa%20is%20a%20medication%20used,decarboxylase%20inhibitor%20class%20of%20drugs.

31. Moore, J. J. (2022, May 2). *Selegiline*. StatPearls - NCBI Bookshelf. https://www.ncbi.nlm.nih.gov/books/NBK526094/

32. *Parkinson's Disease & Medications*. (n.d.). Cleveland Clinic. https://my.clevelandclinic.org/health/diseases/9198-medications-for-parkinsons-disease

33. Mittur, A., Gupta, S. K., & Modi, N. B. (2017). Pharmacokinetics of Rytary®, An Extended-Release Capsule Formulation of Carbidopa–Levodopa. *Clinical Pharmacokinectics*, *56*(9), 999–1014. https://doi.org/10.1007/s40262-017-0511-y

34. *How it Works | RYTARY® (carbidopa and levodopa) extended-release capsules*. (n.d.). https://rytary.com/how-rytary-is-thought-to-work

35. Margolesky, J., & Singer, C. (2018). Extended-release oral capsule of carbidopa–levodopa in Parkinson disease. *Therapeutic Advances in Neurological Disorders*, *11*, 175628561773772. https://doi.org/10.1177/1756285617737728

36. Białecka, M., Kurzawski, M., Klodowska-Duda, G., Opala, G., Jankovic, J., & Droździk, M. (2008). The association of functional catechol-O-methyltransferase haplotypes with risk of Parkinson's disease, levodopa treatment response, and complications. *Pharmacogenetics and Genomics*, *18*(9), 815–821. https://doi.org/10.1097/fpc.0b013e328306c2f2

37. Cheshire, P. A., Bertram, K., Ling, H., O'Sullivan, S. S., Halliday, G. M., McLean, C., Bras, J., Foltynie, T., Storey, E., & Williams, D. R. (2013). Influence of Single Nucleotide Polymorphisms in COMT, MAO-A and BDNF Genes on Dyskinesias and Levodopa Use in Parkinson's Disease. *Neurodegenerative Diseases*, *13*(1), 24–28. https://doi.org/10.1159/000351097

38. Becker, M. L., Visser, L. E., Van Schaik, R. H., Hofman, A., Uitterlinden, A. G., & Stricker, B. H. (2011). OCT1 polymorphism is associated with response and survival time in anti-Parkinsonian drug users. *Neurogenetics*, *12*(1), 79–82. https://doi.org/10.1007/s10048-010-0254-5

39. *Sinemet (carbidopa/levodopa) dose, indications, adverse effects, interactions. . . from PDR.net*. (n.d.). https://www.pdr.net/drug-summary/Sinemet-carbidopa-levodopa-388

40. *What Makes it Different? | RYTARY® (carbidopa and levodopa) extended-release capsules*. (n.d.). https://rytary.com/what-makes-rytary-different?view=paneLvlSteady

41. Haddad, F., Sawalha, M., Khawaja, Y. M., Najjar, A., & Karaman, R. (2017). Dopamine and Levodopa Prodrugs for the Treatment of Parkinson's Disease. *Molecules*, *23*(1). https://doi.org/10.3390/molecules23010040